

The Actual Size of the Air Gap and the Deterioration of Magnetic Core's Properties in Stator Teeth of Induction Motor: Modeling and Analysis of Punching Process Influence

Abstract. The paper deals with results of the numeric modeling of selected parts of the induction motor, whose core consists of punched strips. During modeling, the impact of one of the punching process's parameter, was studied. As it was demonstrated, this parameter has a significant influence on the actual size of the air gap. The necessary data for profile's modeling were obtained from measurements, executed on the rectangular samples.

Streszczenie. Artykuł prezentuje wyniki modelowania wybranych fragmentów silnika indukcyjnego, którego rdzeń wykonano z blach poddanych wykrawaniu mechanicznemu. Podczas modelowania badano wpływ jednego z parametrów charakteryzujących wykrawanie. Jak wykazano, parametr ten ma zasadnicze znaczenie na rzeczywisty rozmiar szczeliny powietrznej silnika. Dane niezbędne do modelowania kształtu profile blach uzyskano z pomiarów wykonanych na prostokątnych próbkach. (Rzeczywisty rozmiar szczeliny powietrznej oraz pogorszenie właściwości obwodu magnetycznego w żebach stojana silnika indukcyjnego: Modelowanie i analiza wpływu wykrawania mechanicznego).

Keywords: punching process, FEM modeling, induction motor

Słowa kluczowe: wykrawanie mechaniczne, modelowanie numeryczne, silnik indukcyjny

doi:10.12915/pe.2014.04.05

Introduction

Accurate modeling of electric motors, despite the use of many different mathematical models (including circuit as well as field models), still requires the use of correction factors that take into account the technological processes implemented during punching and assembling of magnetic core [1]. Research works carried out in this area indicate clearly change of magnetic and energetic properties of ferromagnetic material used in the magnetic core [2-4]. The cause of the changes is for example: pressing the core, the presence of additional internal stresses of the magnetic material structure resulting from locating in the motor frame, shaping of the magnetic circuit by eg. mechanical punching of the single ferromagnetic strip [5-7]. It is known that the main cause of this effect is local degradation of magnetic material, occurring within a few mm from the cut edge. The size of this zone depends on many parameters, such as e.g. the chemical composition of ferromagnetic, used cutting technology, the presence of gas when laser is used, the punching stamp parameters (in the case of punching) [8-10]. As a result of the heat treatment process which should be carried out under controlled temperature during the heating and cooling, it is possible a partial restoration of material properties having degraded internal structure. This process shall be carried out only when it is cost-effective and should be assumed that this is not a common practice. In addition, the internal stress of the material, remained after the punching or laser cutting process, affect the change of ferromagnetic properties. In this case, the microscopic observation of the material internal structure does not indicate a change of grain size or magnetic domains size, while the material properties are different from the properties of the non-destructed one. It is known that the punching tool wear, represented for example by clearance between knives, has an adverse impact on the induction motor parameters too. In fact it is the cause of air gap increase. The knowledge on the possible enlargement of air gap is particularly important for induction motors designers. The author deals with the problem of enlarging air gap, caused the actual cross-section profiles of ferromagnetic strip subjected to punching as well as MMF increase (calculated along the tooth). During the guillotining process carried out on the ferromagnetic samples made of strip with a thickness from 0.35 to 0.6 mm, the clearance of guillotine was controlled and changed.

Experimental activities

During the tests the electrical steel M330-XA was used, where X takes the value 35, 50 and 65 (thickness 0.35, 0.5 and 0.65 mm respectively). This electrical sheet is not fully isotropic and that is why all of the strips (samples) were cut in the same direction in relation to the rolling direction. The measured magnetizing curves of the test sheets of different thickness slightly differ between each other - Fig. 1.

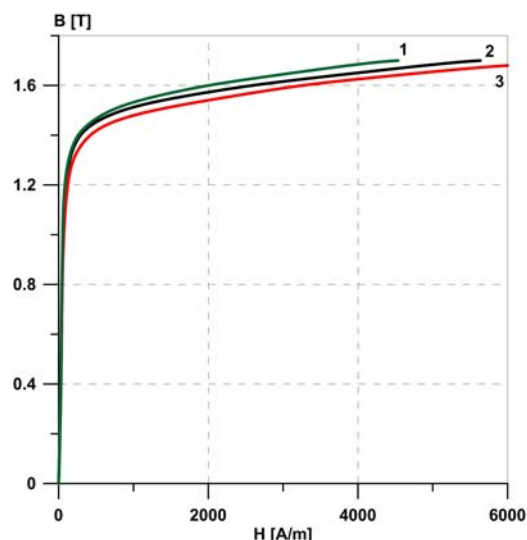


Fig.1. The measured magnetizing curves. 1- M330-65A, 2- M330-35A, 3- M330-50A

The samples were cut using the guillotine, in which it was possible to adjust the size of the clearance between the cutting knives. The clearance size was established in such way to represent different degree of wear of the punching tool. It was assumed that the new cutting tool has a clearance of less than 5% - this value represents the ratio of the clearance size (between the cutting knives) and sheet thickness, whereas the tool worn out has a clearance over 15%. To build a model of the core portion, taking the profiles of cut samples into account, the outlines of shapes were found by measurements. These outlines depend on clearance value of the punching tool used for cutting - Fig. 2. The cut was made for four clearance values: 3%, 5%, 10% and 15% - Fig.3.

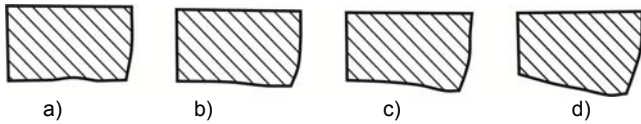


Fig.2. Outlines of shapes used during the FEM models preparation: a- 3%, b- 5%, c- 10%, d- 15%

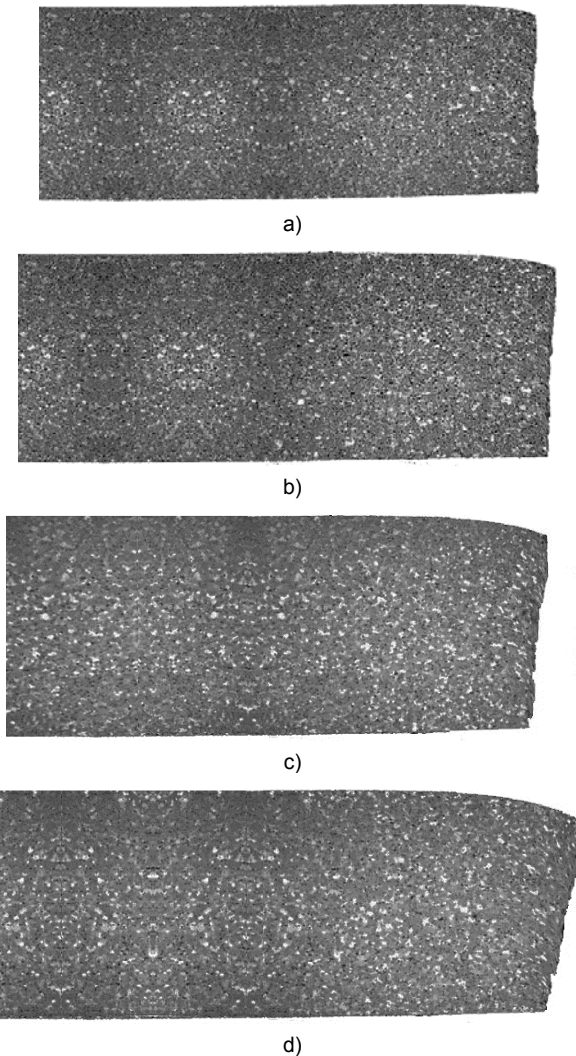


Fig.3. Measured cross sections (profiles) of samples with a clearance: a- 3%, b- 5%, c- 10%, d- 15%

FEM approach and results

The FEM models, representing fragment of the induction motor core, were built in commercial package. Each model contains 20 000 first-order elements – Fig.4. For models representing the fragment of the induction motor core, solving the magnetostatic problem, the assumptions presented below, were adopted: relative magnetic permeability of the core material is equal to $1e6$ (practically in this way the magnetomotive force in the core material was omitted). For comparison, the numerical computation in which the measured magnetizing curve of the magnetic material has been taken into account, were executed. Saturation of magnetic material did not affect in a significant way on the distribution of magnetic field in air gap and did not change the calculations results presented in Tab.1. Calculations were executed for the same average magnetic flux (the magnetic flux was established by enforcing at boundary condition the proper value of the A vector potential). At the top and bottom edge of the accepted

model, $\frac{\partial A}{\partial n} = 0$ was adopted. Calculations were executed

for the three variants of distorted metal profile:
- lack of the profile distortion, resulting from a mechanical cutting,

- distorted profiles of the stator and rotor core sheets,
- distorted profiles of the stator core and mirrored vertically distorted profiles of the rotor core.

Calculations were executed for the three most commonly used thickness of strips: 0.35 mm, 0.5 mm and 0.65 mm, and the air gap size from 0.1 mm to 0.6 mm (most common for a fraction and low power induction motors).

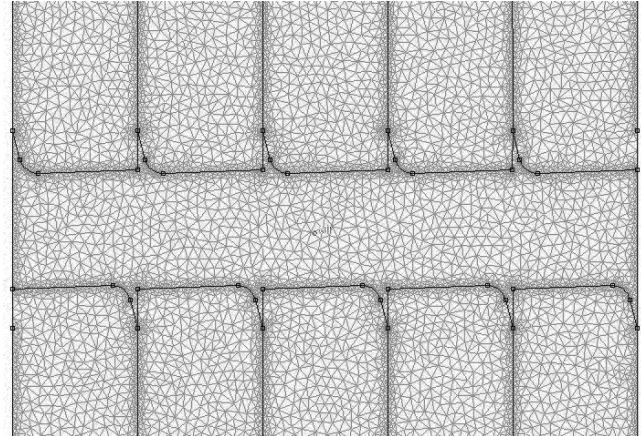


Fig.4. Mesh of the FEM model

When the magnetic flux penetrates the air gap, then the density of the magnetic field energy in i -th elementary volume is described by equation

$$(1) \quad w_i = \frac{B_i H_i}{2}$$

where: B_i , H_i are flux density and field strength at i -th elementary volume respectively.

While the total energy stored in the air gap with the volume V , is given by the formula

$$(2) \quad W = \int_V \frac{B_i H_i}{2} dv$$

Accepting the unitary length of each FEM model, the total energy stored in the air gap can be expressed as

$$(3) \quad W = \int_S \frac{B_i H_i}{2} dS$$

where: B_i , H_i are flux density and magnetic field strength at i -th air gap element respectively, S is the cross-section of the air gap.

If we do not change the profile distortion resulting from cuts, then the surface $S=L \cdot \delta$, where L is the air gap width and δ is its high. So, the magnetic field energy stored in the air gap depends on its high. If the deformation of the sheet profile (resulting from a mechanical cutting) is taken into account, then a change of magnetic field energy stored in air gap is observed. The energy can be represented using the "equivalent" air gap having δ^* height. For the same average induction existing in the air gap (determined by specification of the A vector potential on the edges of the model) then it is possible to write

$$(4) \quad \frac{W}{\delta} \propto B_{av}$$

After necessary transformation, it is possible to write

$$(5) \quad \frac{W}{\delta} = \frac{W^*}{\delta^*}$$

where: W , δ are magnetic field energy and air gap height (for non deformed sheet profile) respectively, whereas W^* , δ^* are magnetic field energy and “equivalent” air gap height (for deformed sheet profile) respectively. Results of executed calculations are presented in Tab.1. Direct estimation of the equivalent air gap’s size, applying profiles presented in Fig. 2, is impossible. It is necessary to perform the calculations using the FEM model, because as a result of the outline’s deformation, appear areas in the air gap, those the magnetic field do not penetrate. Then, the magnetic field energy of these areas is small compared with the energy of the neighboring areas of the air gap – Fig.5.

Table 1. The ratio δ^*/δ calculated for some air gap heights and strip thickness

Clearance [%]	Strip thickness [mm]		
	0.35	0.50	0.65
$\delta = 0.10$ mm			
3	1.057	1.084	1.111
5	1.112	1.160	1.205
10	1.251	1.350	1.446
15	1.389	1.539	1.680
$\delta = 0.30$ mm			
3	1.019	1.028	1.034
5	1.038	1.055	1.070
10	1.086	1.122	1.158
15	1.134	1.191	1.247
$\delta = 0.45$ mm			
3	1.012	1.018	1.023
5	1.025	1.036	1.047
10	1.057	1.083	1.106
15	1.090	1.128	1.165
$\delta = 0.60$ mm			
3	1.009	1.013	1.017
5	1.019	1.027	1.035
10	1.043	1.062	1.080
15	1.067	1.096	1.124

where: δ^* is the equivalent air gap thickness for distorted profile, δ is the air gap thickness for non distorted profile.

The results of the calculations indicate that the increase of the air gap width, determined for non wear tool (clearance 3%) ranges from 0.9% (thickness of air gap 0.6 mm) to 11% (thickness of air gap 0.1) whereas and for heavily wear tool (clearance 15%) it ranges from 6.7% (thickness of air gap 0.6 mm) to 68% (thickness of air gap 0.1 mm). On the basis of the carried out calculations, it can be concluded that the height increase of the air gap (in mm) is following: 1.65% of the strip thickness for clearance 3%; 3.2% for clearance 5%; 7.3% for clearance 10%; 11.5% for clearance 15%. The enlargement of the air gap size seems to be the same for profiles with and without a vertical mirror. The impact of clearance’s size, which is the cause of the air gap increase, can be estimated on the basis of the carried out calculations. The author proposes to adopt the average factor, common for many thickness of strips, air gap’s height and clearances, analyzed in this paper. The equivalent air gap size can be determined by following formula

$$(6) \quad \delta^* = \delta \left(1 + \frac{0.00657 d c}{\delta} \right)$$

where: d is thickness of magnetic strip [mm], c is clearance [%], δ is air gap’s height [mm] (specified for non deformed profile).

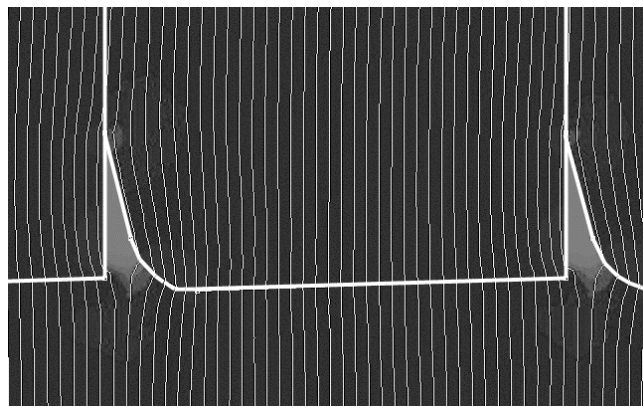


Fig.5. Equipotential lines in a part of FEM model

Another issue considered in the paper is a definition of the magnetomotive force increase, measured along the stator or rotor tooth height, resulting from the partial destruction of the magnetic material. Due to the presence of many different shapes of stator teeth, the analysis will be limited to the simplest shape which is rectangular one. In the case of rotor teeth, the diversity of shape is even greater, what suggests to conduct the analysis for each particular shape separately. The analysis presented is of a general nature, indicating the size of the teeth for which during modeling it is necessary to take into account effects of material destruction, resulting from punching. For sheet type M330-50A, rectangular bars with dimensions 500x120 mm and 500x15 mm were cut, and then laboratory tests have been carried out. On the basis of an analysis of the metal bar profile, it was found that the cutting tool clearance was 4-5%. It was assumed, that the material characteristics of the single rectangular bar (500x120 mm) represent undamaged material, whereas the material characteristics of the sample containing 8 narrow bars (500x15 mm each), represent partially damaged material. The measured material curves, take into account the partial destruction of the material, whose volume is comparable to the volume of undamaged material. In the actual electric motor, flux density in the teeth, exceeds the value of the 1 T and therefore only a fragment of the magnetizing curve representing damaged material, was calculated. The width of the damaged zone and its properties, were estimated using the analytical method described in [11] and next checked by numerical method described in [12]. Based on the results of experiments described in the available literature, it can be concluded that the damaged material has far worse magnetic parameters in comparison with the undamaged material (especially for the flux density lower than 1T for investigated material). At the first step of numerical calculations, the minimum width of the damaged material was estimated. In the FEM model author suggests to make following assumptions: flux density is near 0 in the damaged zone. Due to measurement done, the magnetic field strength was known (for defined flux density). Because in punched strip there are regions with different magnetic properties, then measured flux density (estimated by voltage induced in measuring coil) represents flux density averaged over cross section of the strip. Changing the width of the damaged zones in the FEM model, the minimum ϵ error was achieved. The error was defined by following equation

$$(7) \quad \varepsilon = \frac{\sqrt{\left(B_{av} - \frac{1}{n} \sum_{i=1}^n B_i \right)^2}}{B_{av}}$$

where: n is the number of elementary areas in the cross section of modeled sample, B_i is the calculated flux density at i -th elementary area, B_{av} is the expected average value of the flux density. On the basis of the calculations performed, it was found that the minimum width of the damaged zone near the cut edge is equal to 1.6 mm. Next, the second stage of calculation algorithm was executed. The whole procedure is described in details in [12]. We should keep in mind, that the proposed zone width estimation method, will allow us to estimate the equivalent width of the material having properties independent on the distance from the cut edge. Accepted assumption leads to a situation in which we have a "green" piece of material having properties marked as A and next to it the damaged material having properties marked as B . In the contact area of these materials there is discrete change in material properties. The consequence of this is discrete change e.g. in flux density or specific loss. In fact, the change of the material properties are not discrete but continuous [13]. In this case, it is permissible for the adoption of a model in which there is the equivalent width of the area damaged because the analyzed quantities are integral quantities.

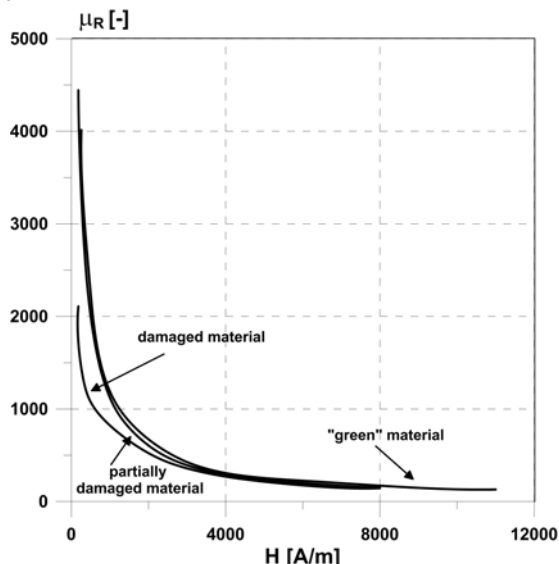


Fig.6 Measured magnetizing curves for "green", damaged and partially damaged material (the sheet type M330-50A)

Using mentioned calculation procedure, the estimated width of the damaged zone, for the tested material is 2 mm. The analytical method used, contains simplifying assumptions, but results obtained with this method are comparable with results obtained by numerical method [14]. The results, in the form of a curves that represents the relative permeability as a function of the maximum field strength value, are shown at Fig. 6. On the basis of measurements, the maximum field strengths were specified, those are necessary to generate specified flux density (averaged over cross section). Sample results are as follows: average flux density 1.5 T – maximum field strength 2362 A/m; average flux density 1.1 T - maximum field strength 290 A/m; average flux density 1 T - maximum field strength 180 A/m. In relation to "green" material, a significant increase of the field strength occurs, necessary to obtain specified flux density value. Higher field strength will cause higher flux density in undamaged part of

material. And, for average induction 1.5 T – flux density in undamaged part of material will reach 1.56 T; for average induction 1.1 T – flux density in undamaged part of material will reach 1.32 T. As a result of the flux density increase in undamaged material part as well as significant increase of specific loss in damaged part (having regard to the less flux density in this part), there will be a rise in iron loss in motor element (stator tooth).

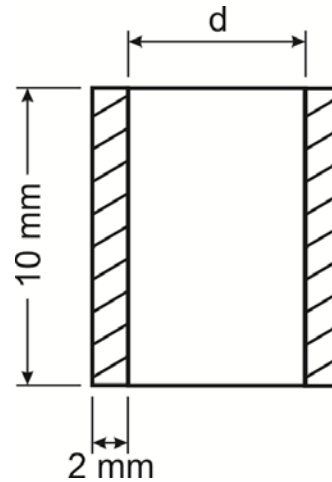


Fig. 7 Dimensions of the tooth (hatched field indicates a damaged material)

The final result of the estimation process, executed for the damaged zone, are relative magnetic permeabilities, computed for the damaged and undamaged areas. Examples results of the calculations are as follows:

- average flux density 1.5 T - $\mu_{RAV} = 507$, $\mu_{R1} = 528$,
 $\mu_{RX} = 449$
- average flux density 1.1 T - $\mu_{RAV} = 3034$, $\mu_{R1} = 3641$,
 $\mu_{RX} = 1360$

where: μ_{RAV} is the relative magnetic permeability determined for average flux density (the sample has damaged and undamaged parts); μ_{R1} is the relative magnetic permeability of undamaged part of sample, subjected to field excitation corresponding to partly damaged sample; μ_{RX} is the relative magnetic permeability of damaged part of sample (according to analytical method described in [11]).

Table 2 The calculated magnetomotive force along the tooth

Average flux density [T]	1.5	1.6	1.7	1.8
The total width of the tooth - 14 mm				
MMF [A]	13.6	28.0	54.0	81.0
The total width of the tooth - 12 mm				
MMF [A]	13.7	28.1	54.0	81.0
The total width of the tooth - 10 mm				
MMF [A]	15.4	33.0	60.0	87.0
The total width of the tooth - 8 mm				
MMF [A]	19.0	40.0	68.0	96.0
The total width of the tooth - 6 mm				
MMF [A]	29.0	56.0	84.0	112.0

Knowing the relative magnetic permeability curve, calculated for the damaged material as well as estimated width of the damaged zone, calculations of MMF along the tooth model, were executed. The FEM model of the tooth was built. Modeled tooth had rectangular shape and the overall width in range from 6 mm to 14 mm. The damaged zone width equal to 2 mm was taken into account. The height of the model was fixed at 10 mm and not changed with the

change of the tooth width (Fig. 7). Calculations were executed for the four average flux density values: 1.5 T, 1.6 T, 1.7 T, 1.8 T. In built FEM model the non-linear magnetization curves, representing "green" and damaged material, were used. Table 2 and Fig. 8 present the results of the calculations. As a result of destructed zone consideration, the MMF increases of about 25% to 100%.

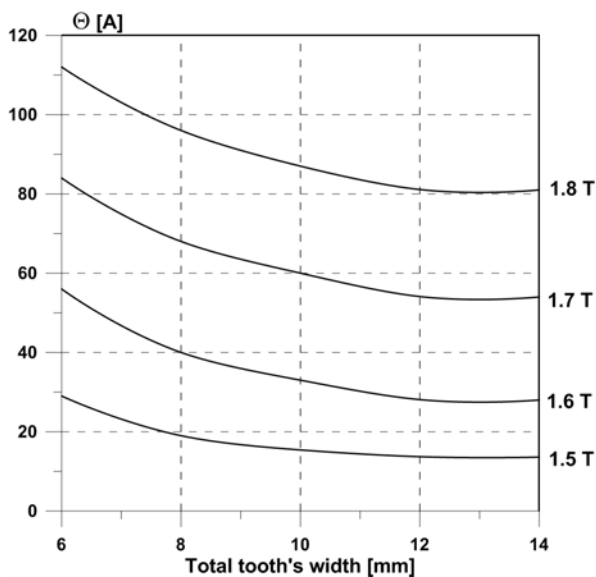


Fig.8 Magnetomotive force vs. tooth's width

Conclusions

The paper presents the results of the measurements and computer simulations, concerning some parts of induction motor, subjected to punching process. It has been shown that deformation of the profile of cut strip, is a result of punching. This is the cause of the air gap increase. The impact of damaged material on magnetic flux density distribution in a cross-section of a stator tooth, as well as variation of MMF, were analyzed too. The MMF Increase in the teeth can also be converted to increase of the air gap height. Performed computer simulations and analytical formulas proposed, allow designers of electrical motors, making it easier to assess the situation, where technological factors should be taken into account. The data necessary for calculation were obtained by simple non-invasive measurements. The complete verification of the proposed method needs to be supported by additional research carried out on the analyzed samples; for this reason further experimental investigations are ongoing. However, the obtained results of estimation of the damaged zone width correspond very well with the results of other researchers. According to the author's knowledge, the analytical relationship that allows us to calculate the actual air gap width as a function of the clearance, the thickness of the

sheet and the width of the ideal air gap, there was not yet tested or published.

REFERENCES

- [1] Dems M., Komęza K., Finite-element and analytical calculations of no-load core losses in energy-saving induction motors, *IEEE Transaction on Industrial Electronics*, 59 (2012), 2934-2946
- [2] Wilczyński W., Talik S., Szubzda B., Porównanie wpływu wykrawania i cięcia laserem blach elektrotechnicznych na ich własności magnetyczne, *Przegląd Elektrotechniczny*, (2003), No 2, 160-163
- [3] Belgrand T., Eple S., Tell us about your punch, we'll tell you about your electrical steel magnetic properties, *Journal de Physique*, vol.8, 1998, pp.611-614
- [4] Boglietti A., Cavagnino A., Ferraris L., Lazzari M., The annealing influence onto the magnetic and energetic properties in soft magnetic material after punching process, *Conf. Rec. IEEE-IEMDC'2003*, Madison, Wisconsin, USA,, pp.503-508
- [5] Schoppa A., Schneider J., Roth J.-O., Influence of the cutting process on the magnetic properties of non-oriented electrical steels, *JMMM*, 215-216 (2000), 100-102
- [6] Pulnikov A., Baudouin P., Melkebeek J., Induced stresses due to the mechanical cutting of non-oriented electrical steels, *JMMM*, 245-255 (2003), 355-357
- [7] Baudouin P., De Wulf M., Kestens L., Houbaert Y., The effect of the quillotine clearance on the magnetic properties of electrical steels, *JMMM*, 256, 2003, pp.32-40
- [8] Senda K., Ishida M., Nakasub Y., Yagi M., Influence of shearing process on domain structure and magnetic properties of non-oriented electrical steel, *JMMM*, 304 (2006), e513-e515
- [9] Gomes E., Schneider J., Verbeken K., Pasquarelle G., Houbaert Y., Dimensional effects on magnetic properties of Fe-Si steels due to laser and mechanical cutting, *IEEE Transaction on Magnetics*, 46 (2010), No 2, 213-216
- [10] Pulnikov A., Baudouin P., Dupre L., de Wulf M., Houbaert Y., Melkebeek J., Investigation of local magnetic effects in rotating electrical machines, *Proc. 7 Conf. ELECTRIMACS*, 2002
- [11] Gmyrek Z., Cavagnino A., Analytical method for determining the damaged area width in magnetic materials due to punching process, *Proc. IECON Conf*, 2011, 1764-1769
- [12] Gmyrek Z., Modelling of the properties in soft magnetic material after punching process, *Przegląd Elektrotechniczny*, No 1a (2012), 263-268
- [13] Rygał R., Moses A. J., Derebasi N., Schneider J., Schoppa A., Influence of cutting stress on magnetic field and flux density distribution in non-oriented electrical steels, *JMMM*, 215-216, 2000, pp.687-689
- [14] Gmyrek Z., Cavagnino A., Ferraris L., Estimation of the magnetic properties of the damaged area resulting from the punching process: Experimental research and FEM modeling, *IEEE Transaction on Industry Applications*, 49 (2013), 2069-2077

Authors: dr hab. inż. Zbigniew Gmyrek, Politechnika Łódzka, Instytut Mechatroniki i Systemów Informatycznych, ul. Stefanowskiego 18/22, 90-924 Łódź, E-mail: zbigniew.gmyrek@p.lodz.pl